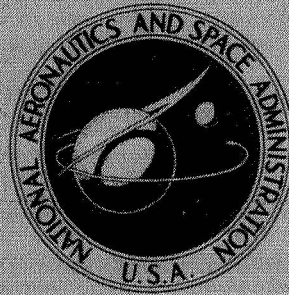


NASA TECHNICAL  
MEMORANDUM



NASA TM X-1955

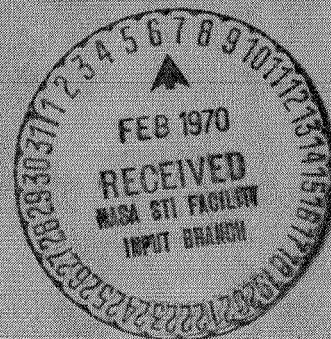
NASA TM X-1955

CASE FILE  
COPY

EVALUATION WITH A TURBOFAN ENGINE  
OF AIR JETS AS A STEADY-STATE  
INLET FLOW DISTORTION DEVICE

*by Willis M. Braithwaite, John H. Dicus,  
and John E. Moss, Jr.*

*Lewis Research Center  
Cleveland, Ohio*



1. Report No. NASA TM X-1955	2. Government Accession No.	3. Recipient's Catalog No.	
4. Title and Subtitle EVALUATION WITH A TURBOFAN ENGINE OF AIR JETS AS A STEADY-STATE INLET FLOW DISTORTION DEVICE		5. Report Date January 1970	6. Performing Organization Code
		8. Performing Organization Report No. E-5325	
7. Author(s) Willis M. Braithwaite, John H. Dicus, and John E. Moss, Jr.		10. Work Unit No. 720-03	11. Contract or Grant No.
9. Performing Organization Name and Address Lewis Research Center National Aeronautics and Space Administration Cleveland, Ohio 44135		13. Type of Report and Period Covered  Technical Memorandum	
		14. Sponsoring Agency Code	
12. Sponsoring Agency Name and Address National Aeronautics and Space Administration Washington, D. C. 20546			
15. Supplementary Notes			
16. Abstract An experimental program has been conducted at the Lewis Research Center to evaluate the effectiveness of the secondary-air jet distortion device. This system is compared with the conventional screens as a means of creating a 180° distortion. The results are presented in terms of engine stall limits and inlet profiles. The two systems produced essentially equivalent distortion profiles at a Reynolds number index of 0.5. The stall-limited distortions, determined with screens and air jets, were in good agreement.			
17. Key Words (Suggested by Author(s)) XXXXXXXXXXXXXXXXXXXX		18. Distribution Statement Unclassified - unlimited	
19. Security Classif. (of this report) Unclassified	20. Security Classif. (of this page) Unclassified	21. No. of Pages 28	22. Price* \$3.00

\* For sale by the Clearinghouse for Federal Scientific and Technical Information  
Springfield, Virginia 22151

# EVALUATION WITH A TURBOFAN ENGINE OF AIR JETS AS A STEADY-STATE INLET FLOW DISTORTION DEVICE

by Willis M. Braithwaite, John H. Dicus, and John E. Moss, Jr.

Lewis Research Center

## SUMMARY

Many problems have been encountered in the development of propulsion systems for new, high-performance supersonic aircraft. A major problem area has been in achieving stability in the propulsion system. Inadequate understanding of the flow field at the discharge of the inlet and its effect on engine stability has contributed to this problem.

An experimental program has been undertaken at Lewis to obtain a better understanding of this problem. As part of this program, a versatile distortion device has been developed utilizing air jets. This report compares the effectiveness of the air jets with the conventional screens as a means of creating distortion. These results are presented in terms of total pressure, Mach number, and  $(\text{TRMS } \Delta P)/P$  profiles and engine stall limits produced by the inlet distortions. The two systems produced essentially equivalent  $180^\circ$  distortions at a Reynolds number index of 0.5. The stall-limited distortions, determined with screens and with air jets, were in good agreement.

## INTRODUCTION

Many problems have been encountered in the development of propulsion systems for new, high-performance supersonic aircraft. A major problem area has been in achieving stability. These problems resulted from inadequate understanding of the flow field at the discharge of the supersonic inlet and its effect on engine stability (refs. 1 to 5).

An experimental study of the effects of steady-state and dynamic compressor inlet disturbances on the operating limits of turbine engines has been undertaken at Lewis. For this program, a two-spool turbofan engine typical of those used in supersonic aircraft was selected. High-response pressure measurement capability was developed (ref. 5) to determine the occurrence of stall and its progression through the compressor.

Steady-state airflow distortions have been created in previous investigations by the

use of screens ahead of the compressor face (refs. 1 and 2). The use of screens, while giving good steady-state distortions, is undesirable because of the time required to change screens in an altitude facility. Also, screens are not suitable for creating time-variant flow disturbances.

A means of creating flow distortions, both steady state and time variant, by the use of air jets in the inlet duct ahead of the engine has been developed at Lewis (ref. 6). The effect of this device on engine performance for both uniform and distorted steady-state flow is presented in this report. These results are compared with those obtained using screens with the same engine (ref. 7).

Data were obtained for a Reynolds number index of 0.5 for a range of inlet airflows. The results are presented in the form of compressor operating lines, stall limits, rotor speed matches, and inlet pressure profiles.

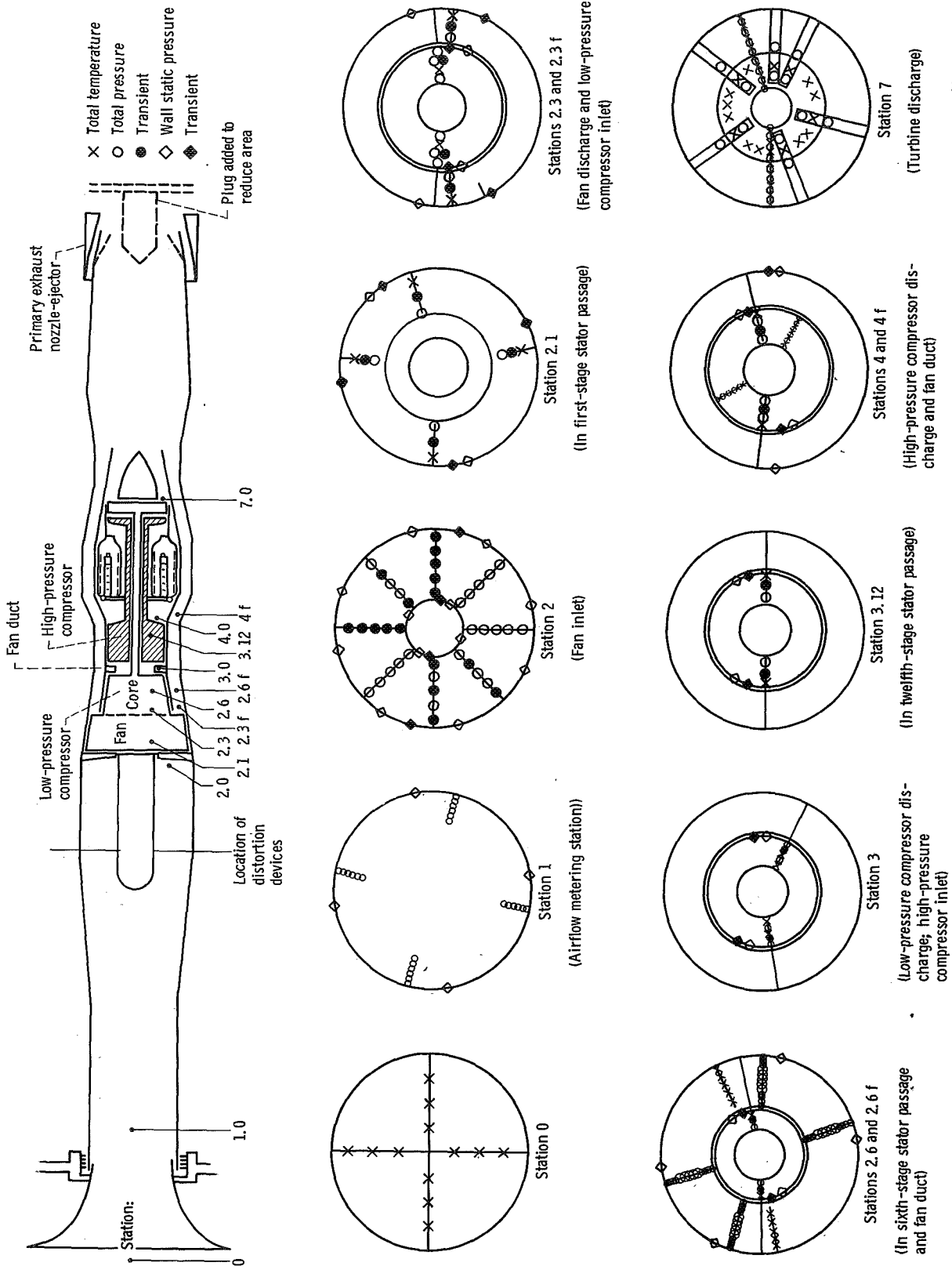
## APPARATUS

The engine, instrumentation, and inlet airflow distortion devices are discussed in this section. A brief description is also given of the engine installation in the facility.

### Engine

The engine used for this investigation was a nonstandard Pratt & Whitney TF30-P-1 twin-spool turbofan. The compressors and combustor section were standard production P-1 items, while the turbine and afterburner-tailpipe were of a preproduction configuration. The preproduction turbine would cause the low pressure compressor to have a slightly higher operating line (approx 2 percent). Therefore the data obtained with this engine would indicate valid trends, but not necessarily levels, of performance typical of production P-1 engines.

The physical layout of the engine, shown schematically in figure 1, consists of a three-stage axial-flow fan mounted on the same shaft with a six-stage axial-flow, low pressure compressor. This unit is driven by a three-stage, low pressure turbine. A seven-stage, axial-flow compressor driven by a single-stage, air-cooled turbine makes up the high-speed spool. The nominal overall pressure ratio of the compressor system is 17:1 with a fan bypass ratio of 1. The fan duct airflow is diverted from the core flow by a splitter ring at the exit of the third-stage rotor. It then passes through an annular passage surrounding the core engine and is combined with the turbine discharge gases at the afterburner inlet. The total flow is then discharged through a variable-area exhaust nozzle. An ejector nozzle, having aerodynamically operated blow-in doors and exit leaves, is a part of the normal engine-afterburner assembly. The ejector controls the



CD-10308-14

Figure 1. - Instrumentation layout.

expansion of the primary jet and pumps cooling and purging air for the engine compartment.

The engine was also equipped with automatic 12th-stage bleeds. These bleeds opened at low engine speeds to aid in acceleration and closed when the pressure rise across the low compressor reached a predetermined value.

Engine modifications. - Several modifications were made to make this engine more suitable for this investigation. The afterburner fuel system was deactivated, and the afterburner portion of the control was modified such that the primary exhaust nozzle area could be increased independently from full closed, or rated, to full open (193 percent of rated). A plug, not supported by the engine, could be inserted into the nozzle to reduce the area to 72 percent of rated. The blow-in doors and exit leaves were removed from the ejector.

The 12th-stage bleeds were also modified such that they could be placed on automatic operation or could be maintained either in the open or closed position as desired. This permitted obtaining data with the bleeds closed at low speeds and open at high speeds, which would not be possible in the automatic configuration.

Another modification was the incorporation of a fuel-step device. An accumulator, which filled with fuel during normal operation, was discharged rapidly by pressurizing it with high-pressure gaseous nitrogen. The fuel was injected into the fuel system between the engine and the fuel control. The size of the step could be controlled by the gas pressure and the length of time that it was supplied to the accumulator.

Engine protection systems. - The danger of damage to the engine resulting from exceeding the turbine inlet temperature or rotor speed limits was minimized by modifying the engine control which schedules fuel flow as a function of burner pressure. A three-way valve, inserted in the burner pressure sensing line to the control, was actuated whenever one of these limits was exceeded. This action vented the control to test chamber pressure (approx. one-sixth of atmospheric pressure). The control then reduced the fuel flow to a minimum value. The engine is normally equipped with an automatic relight switch which activates the ignition circuit if the primary combustor blows out. It detects a rapid decrease in burner pressure. This circuit was also modified such that the switch activated the three-way valve instead of the igniters. Thus, the fuel flow was reduced to the minimum when compressor stall caused a pressure collapse at the compressor discharge. Visual and audible alarms were also triggered by each of these detectors.

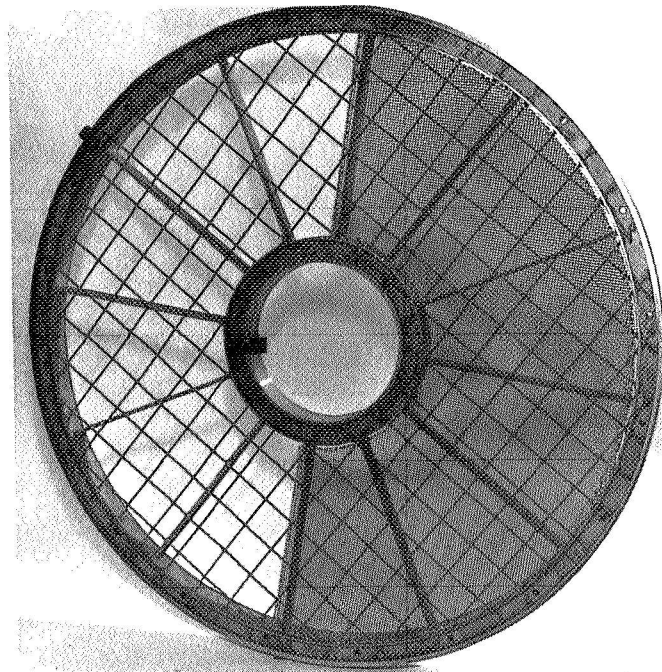
## Instrumentation

The instrumentation used in this investigation was basically the same as that used in preceding TF30-P-1 investigations (refs. 5 and 7). The station identification and probe

locations are shown in figure 1. The stations were selected to divide the compressor into groups of three or four stages. At each station the instrumentation was located in the left and right sides of the engine providing the capability for evaluating both the distorted and undistorted compressor performance.

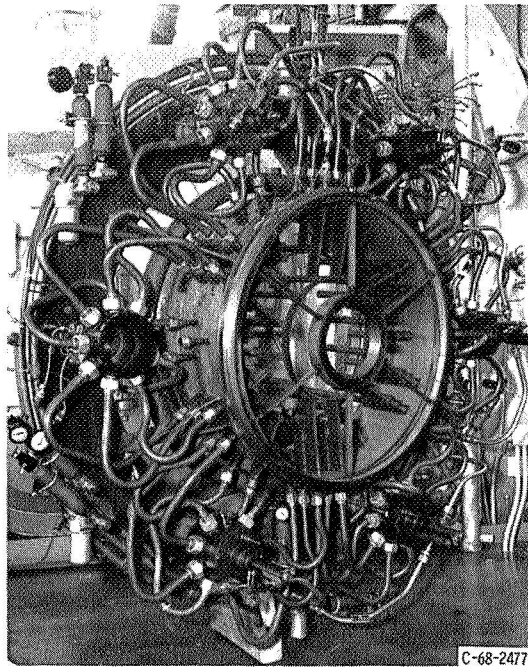
Steady-state instrumentation. - Pressures were recorded on a digital, automatic, multiple-pressure recorder having three pressure ranges: (1) zero to 14 psia $\pm$ 0.014 psi (9.6 N/cm<sup>2</sup> abs $\pm$ 0.0096 N/cm<sup>2</sup>), (2) zero to 35 psia $\pm$ 0.035 psi (24 N/cm<sup>2</sup> abs $\pm$ 0.024 N/cm<sup>2</sup>), and (3) zero to 140 psia $\pm$ 0.014 psi (96 N/cm<sup>2</sup> abs $\pm$ 0.096 N/cm<sup>2</sup>). Shielded Chromel-Alumel thermocouples were used to measure all temperatures and were recorded on an automatic voltage digitizer. These systems are described in more detail in reference 8.

High-response transient instrumentation. - The number of transient probes and their location are shown in figure 1. This instrumentation was designed to have a frequency response to approximately 300 hertz with a maximum of  $\pm$ 5 percent error in amplitude and is described in reference 5. This required the use of small transducers capable of being located within  $1\frac{1}{2}$  inches from the sense point. Thus, most of the transducers were within the engine envelope and subject to a hostile temperature environment. The design and methods of cooling and calibration of these transducers is discussed in the appendix. A steady-state pressure measurement was made adjacent to each transient measurement. This steady-state measurement provided steady-state data in addition to the initial value for the transient measurement.

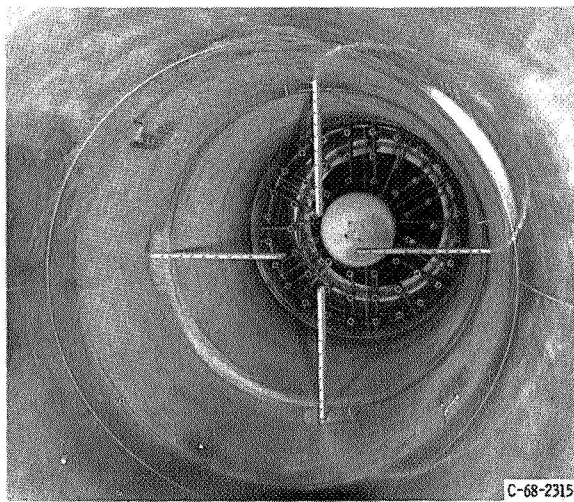


C-68-1305

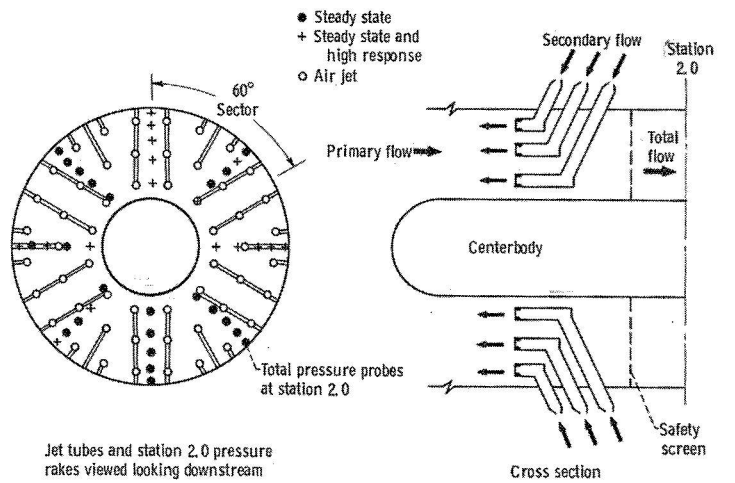
Figure 2. - Typical distortion screen, looking downstream.



(a) Spoolpiece (looking upstream: showing tubes, valves, and jets).



(b) Air jets viewed through inlet bellmouth.



(c) Schematic drawing of system.

Figure 3. - Air-jet distortion hardware.

## Distortion Devices

Variations in total pressure at the compressor face were obtained in two ways. The first way made use of screens blocking part of the inlet duct. A typical screen and support are shown in figure 2. The degree of distortion was controlled by varying the mesh and wire size of the screen. The screen sizes used are given in reference 7.

The second method of creating nonuniform total pressure at the compressor face was to inject jets of air into the inlet duct in a direction counter to the primary airstream. This resulted in the cancellation of part of the momentum of the primary stream and a loss in total pressure. This device, developed at Lewis (ref. 6) consisted of 54 individual jets divided into six groups of nine each (fig. 3). A remote-controlled hydraulically operated valve governed the flow through each group of nine jets, each group covering a  $60^\circ$  sector of the inlet annulus. Therefore, depressed pressure patterns of  $60^\circ$ ,  $120^\circ$ ,  $180^\circ$ ,  $240^\circ$ , or  $300^\circ$ , or combinations thereof, could be obtained. The degree of pressure depression was controlled by the rate of airflow through each jet sector. Each jet was operated at a pressure ratio above that required to choke the exit throat, which had an area of 0.44 square inches ( $2.84 \text{ cm}^2$ ). Therefore the desired degree of distortion could be obtained easily and quickly during the test by varying the flow control valve area and/or the supply pressure to the valves (i. e., the pressure upstream of the jet orifice).

To protect the engine from foreign-object damage, a 0.855-inch (2.17-cm) screen of 0.105-inch (0.2667-cm) diameter wire was positioned across the inlet duct between the engine and the jet device. This screen was located approximately two-thirds of a duct diameter ahead of the engine face just behind the jet spoolpiece. A more complete description of the jet system and its operation is given in reference 6.

## Engine Installation

The engine was installed in an altitude test chamber (fig. 4). The installation was a conventional direct-connect type. The altitude chamber includes a forward bulkhead separating the inlet plenum from the test chamber. Conditioned air was supplied to the plenum at the desired pressure and temperature. The chamber aft of the bulkhead was evacuated to the desired altitude pressure. The conditioned air flowed from the plenum through a bellmouth and duct to the compressor inlet. It was in this duct that the distortion devices were placed. A valve in the bulkhead allowed some of the air to bypass the engine. This valve was automatically controlled to maintain a constant inlet pressure and ram-pressure ratio across the engine during steady-state and normal engine transient operation. The exhaust from the engine was captured by a collector extending

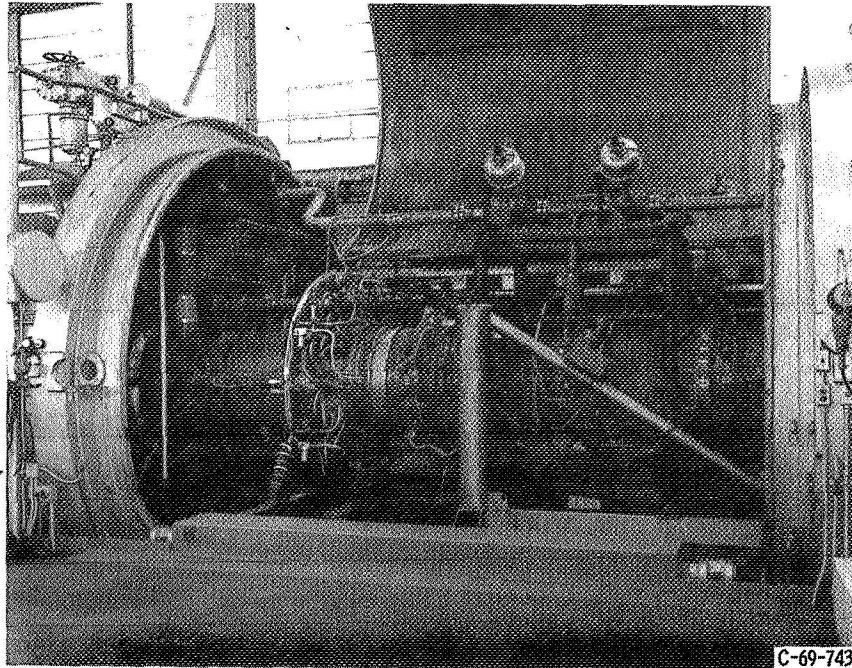


Figure 4. - Engine installed in altitude facility, showing air-jet hardware.

through a rear bulkhead, which minimized the recirculation of exhaust gases into the test chamber. The exhaust, and thus chamber, pressure was controlled by an automatic valve.

## PROCEDURE

### Test Conditions

This investigation was conducted at an engine inlet Reynolds number index of 0.5. It was not possible to control the temperature of the high-pressure air supplied to the jets (secondary airflow). Therefore the inlet air temperature was matched to the secondary-air temperature and varied from approximately 60° F (16° C) to 90° F (32° C). The inlet total pressure, as measured in the undistorted sector of the compressor face, was adjusted to maintain the 0.5 Reynolds number index.

Ram-pressure ratio across the engine was held greater than 3:1 to assure a choked exhaust nozzle at all operating conditions. For this investigation, the exhaust nozzle usually was not varied and all interstage compressor bleeds were locked in the closed position, except where noted.

## Stall Data

The stall limits for the compressor resulting from distorted inlet flow were obtained by slowly increasing the degree of distortion until complete compressor stall occurred. Only a  $180^\circ$  circumferential-step distortion pattern was used for this investigation as the primary purpose was to evaluate the air-jet system by comparison with similar screen data.

Screens. - The limits were obtained with a given screen by slowly accelerating the engine from idle speed until stall occurred. The low-rotor speed was noted. This condition was repeated with the 12th-stage bleeds open, permitting measurement with the steady-state instrumentation, of the inlet distortion that caused the compressor to stall when the bleeds were closed. The screen was then replaced with one of greater solidity and the process repeated until a stall limit was obtained near the idle speed.

Air jet. - The inlet airflow distortion was created by flowing a constant small amount of secondary air through three valves ( $180^\circ$  sector). The low flow was necessary as these were not positive shutoff valves. The distortion was then slowly increased by slowly opening the remaining three valves until complete compressor stall occurred. The corrected inlet airflow was held constant by holding constant low-rotor speed, and the 12th-stage bleeds were closed. When stall occurred, the pressure at the valve discharge was noted and the process repeated with the 12th-stage bleeds open in order to obtain a steady-state measurement of the limiting distortion at that corrected airflow. Other airflows (corrected low-rotor speeds) were selected and the limits found in the same manner.

## RESULTS AND DISCUSSION

### Uniform Inlet Flow

An air-jet system was developed to create flow distortions at the compressor face. It was considered that the presence of the jet hardware in the duct alone would create some distortion; thus, this hardware was designed for a minimum disturbance of the flow and as little distortion as possible. The first part of this investigation was to determine what effect on performance and stall limits the hardware itself had. A second factor would be the disturbance or distortion resulting with all the jets flowing uniformly. Distortion could result from nonspreading of the jets, especially at high secondary flow rates. The mixing of the airstreams could also produce random pressure fluctuations. Both of these effects resulting from the secondary flow could effect the stall limits and steady-state performance of the engine.

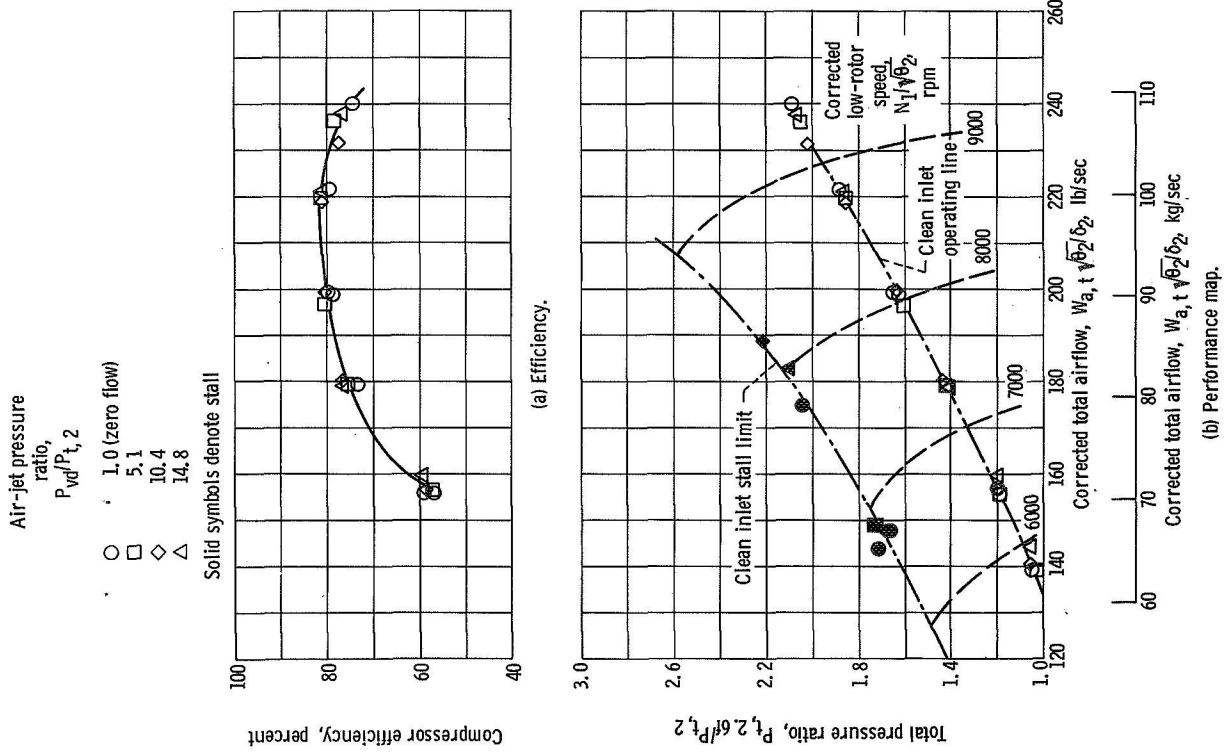


Figure 5. - Effect of air-jet hardware and uniform secondary flow on performance of tip section of the fan.

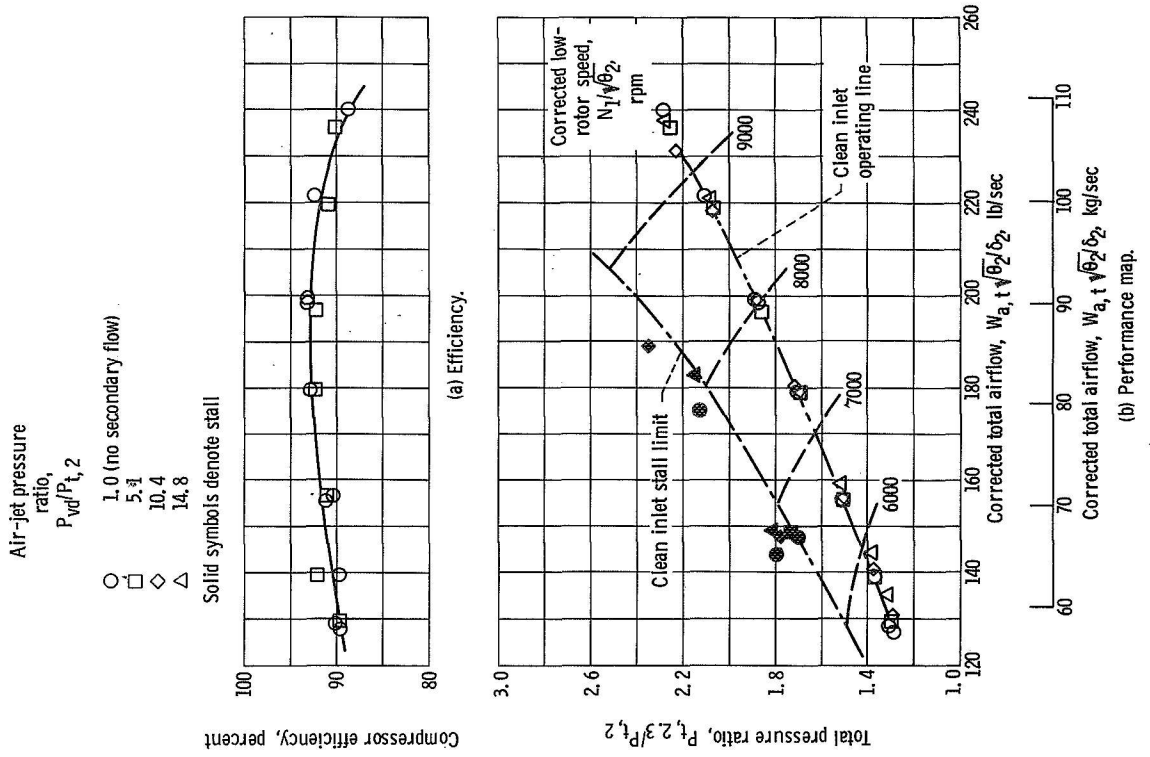


Figure 6. - Effect of air-jet hardware and uniform secondary flow on performance of hub section of the fan.

The first part of the investigation was conducted to determine the effects of the presence of the hardware without secondary flow and of uniform secondary flow on the steady-state performance and stall limits of the engine. Resulting data are presented in plots of compressor efficiency and total pressure ratio as a function of corrected airflow for the compressor units in figures 5 to 8. Data are presented for only rated exhaust nozzle area (normal engine operating line). The fan is considered to be the first three stages. This is divided into two units, tip and hub sections, as defined by the total pressure ratios (1) from the fan duct aft of the third stage (tip) to inlet and (2) from the inlet of the fourth stage to engine inlet at the hub section. The low pressure compressor is defined as the fourth through ninth stage and the high pressure compressor as the 10th through 16th stage. The rotor speed matches are presented in figure 9 for the three basic compressor units as functions of high-rotor speed corrected by the inlet total temperature.

Data are presented for operation without the jet hardware, with the hardware but no secondary flow, and for three levels of uniform secondary flow. There was no significant effect of either the jet hardware or uniform secondary flow on the engine steady-state operating line, efficiencies, or corrected rotor speed matches. Although the stall-limit data are meager, there was no indication of any effect on the limit or stall margin. This is also based on the ability to operate the engine under steady-state conditions over all the speeds and exhaust nozzle areas possible with the clean inlet. Some stalls had been encountered with an  $A_j = 193$  percent of rated and  $N_2/\sqrt{\theta_2}$  of 12 800 rpm with the clean inlet. No such stalls were encountered with the air-jet hardware in place nor with uniform secondary flow.

Total pressure profiles are presented as contour maps in figure 10. These maps are based on curve fitting and interpolating the 40 total pressure measurements at the compressor inlet. Operation with the jet hardware in place but without secondary flow, increased the magnitude of the low-pressure region approximately 1 to 2 percent below the average pressure at  $180^\circ$  and formed a slight depression at  $0^\circ$ . A similar, but smaller distortion is observed at  $90^\circ$  and  $270^\circ$ . As mentioned before, this did not seem to affect the engine performance. These distortions were reduced with a uniform secondary flow through the jets (fig. 10(c)). There is no evidence of distortion resulting from the jet flow patterns. The small distortions resulting from the presence of the hardware in the duct can, therefore, be eliminated by flowing air through the jets.

The random pressure fluctuations at station 2 are presented in figure 11 as the true root mean square (TRMS) amplitude of the random pressure in percent of the mean total pressure as a function of the corrected engine inlet airflow. The TRMS values were electrically measured by a TRMS meter using the output from the 18 high-response transducers (fig. 1). These values were then averaged. The TRMS amplitudes were measured for a frequency band from 0 to 500 hertz. The data obtained in front of the engine with the air jets flowing from zero to maximum flow is within the band for the duct with no hard-

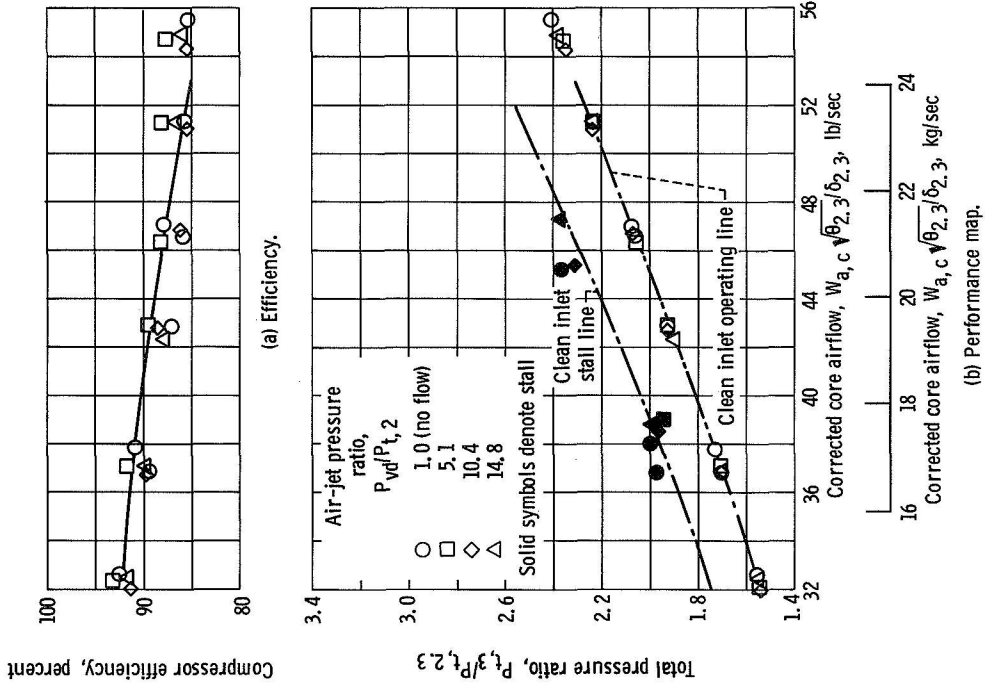


Figure 7. - Effect of air-jet hardware and uniform secondary flow on performance of the low-pressure compressor. Exhaust nozzle area,  $A_j = 100$  percent of rated area.

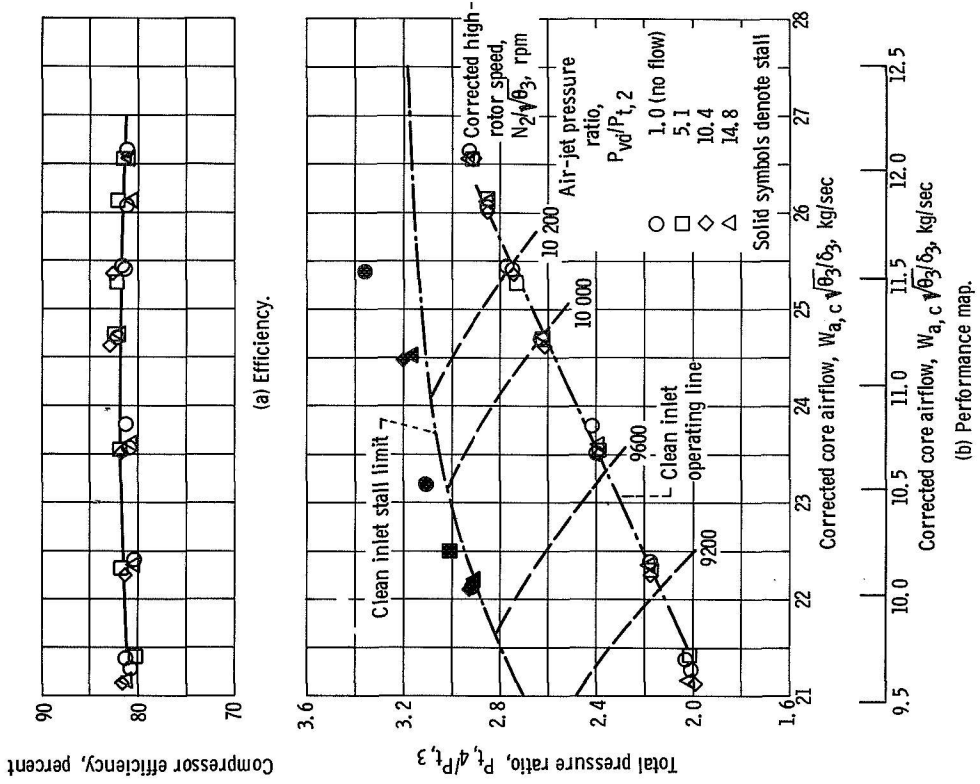


Figure 8. - Effect of air-jet hardware and uniform secondary flow on performance of the high pressure compressor.

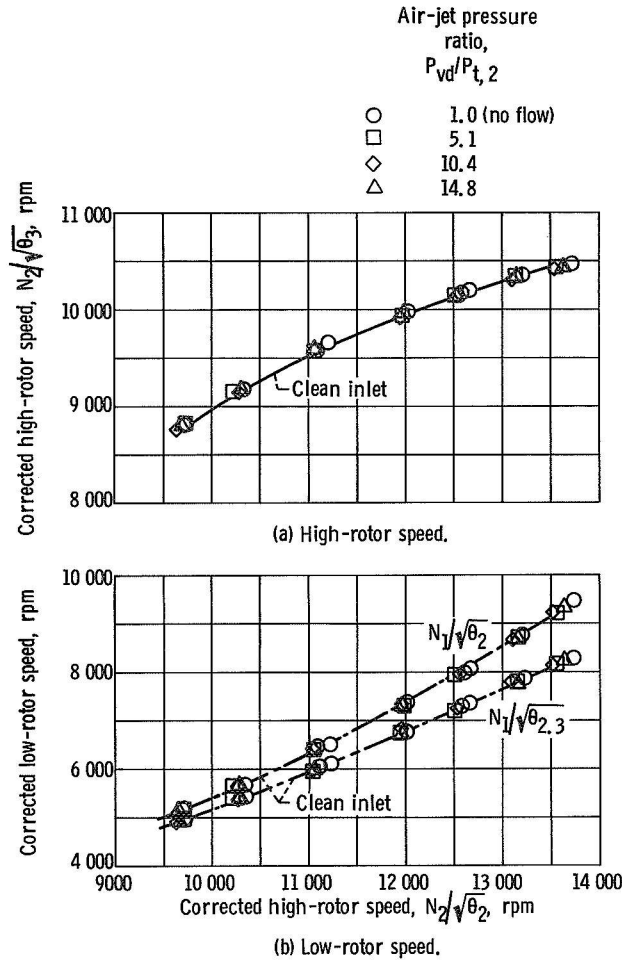
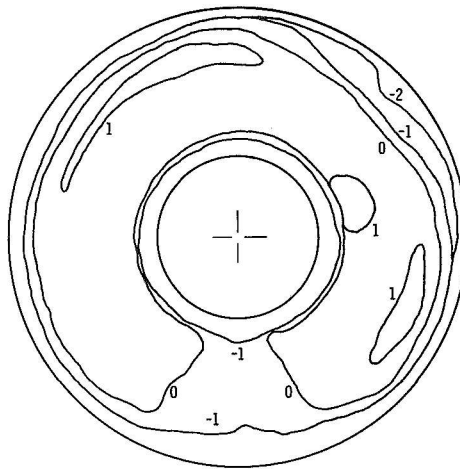


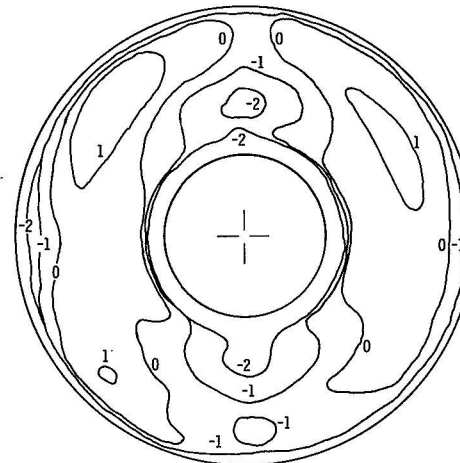
Figure 9. - Effect of air-jet hardware and uniform secondary flow on corrected rotor speed matches.

ware and that obtained with distortion screens. Also shown are data obtained during the calibration of the air jets (ref. 6). The lower values obtained with the engine are believed to be due to the screen placed downstream of the jet hardware for this investigation as the jet data agree with the screen data.

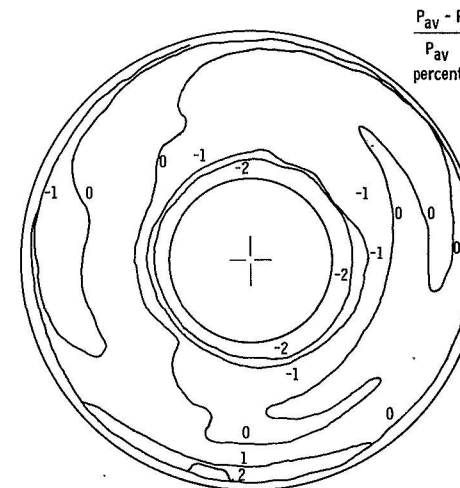
The pressure losses resulting from the air-jet hardware in the duct with and without secondary flow are presented in figure 12. The loss in total pressure from the inlet plenum to compressor face is shown in figure 12(a) as a function of the compressor inlet corrected airflow and ratio of jet pressure to inlet total pressure. The jet pressure was measured by a wall static located at the discharge of the flow control valves. It was assumed that the inlet duct frictional pressure loss was represented by the no-flow case (i. e., when the jet pressure ratio equals 1). The pressure loss resulting from the action of the jets may then be found by dividing the pressure ratios with secondary flow by the



(a) No hardware in duct; corrected total airflow,  $W_{a,t} \sqrt{\theta_2/\theta_1} = 239$  pounds per second (108.5 kg/sec).



(b) Jet hardware, no secondary flow; corrected total airflow, 240 pounds per second (109 kg/sec).



$\frac{P_{av} - P}{P_{av}}$   
percent

(c) Jet hardware and maximum secondary flow; corrected total airflow;  $W_{a,t} \sqrt{\theta_2/\theta_1} = 238$  pounds per second (108 Kg/sec).

Figure 10. - Effect of air-jet hardware and uniform secondary flow on compressor inlet total pressure distribution.

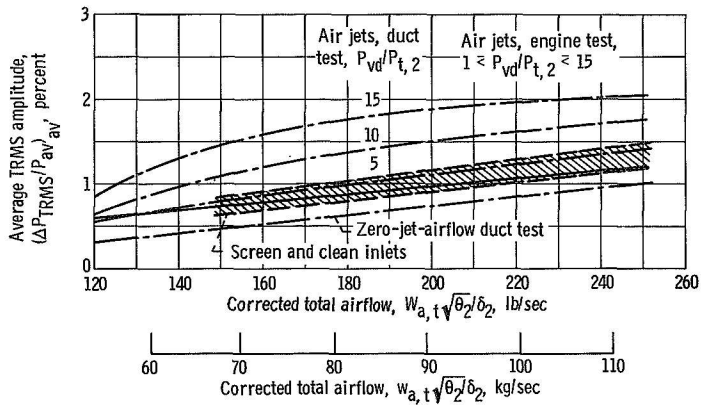


Figure 11. - Random pressure fluctuations at compressor inlet. Average true root-mean-square (TRMS) values are for 18 probes and for a frequency band from 0 to 500 hertz.

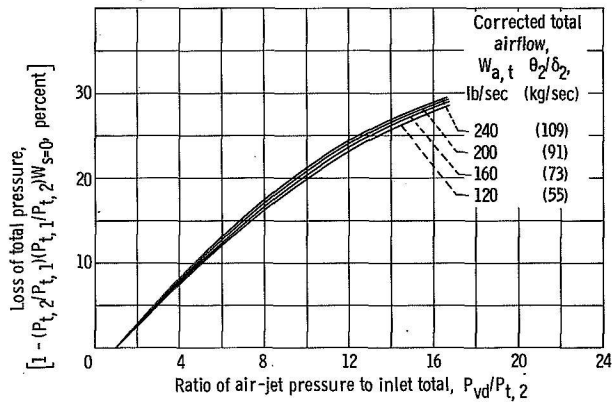
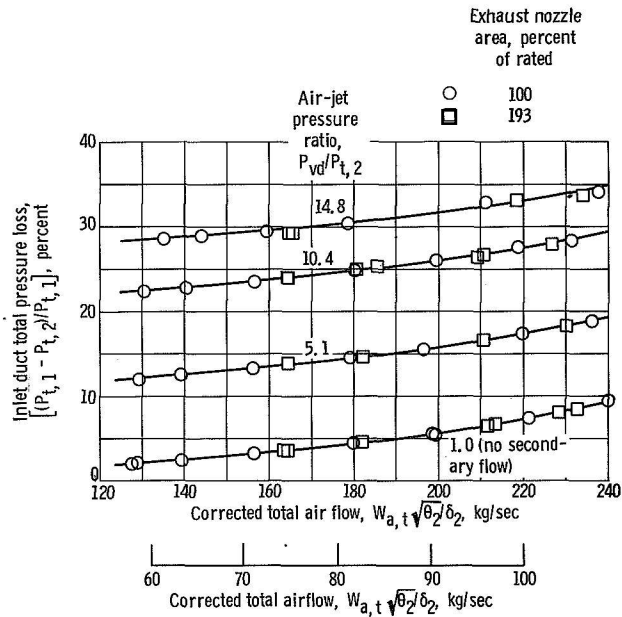


Figure 12. - Total pressure loss resulting from air jets with uniform secondary flow.

no-flow value. This total pressure loss is presented in figure 12(b) as a function of jet pressure ratio. Only a small effect due to primary airflow is evident. Inasmuch as the undistorted total pressure at the compressor face is held constant during testing, the increase in loss due to friction with increasing airflow (or Mach number) results in an increase primarily in the plenum pressure, but has little effect on the momentum loss. Therefore, a distortion resulting from a set jet pressure would remain relatively constant over a range of air-flows (i. e., engine speeds).

## Distorted Inlet Flow

The distortion required to stall the compressor under steady-state operating conditions is presented in figure 13 for a range of corrected inlet airflows. The degree of distortion is presented in terms of  $K_{D2}$ , a parameter developed by Pratt & Whitney for use with the TF30 engines. It is a function of the circumferential extent of the total pressure depression and the differential between the average and minimum total pressures for each ring. A more precise definition is given in appendix B. (Symbols are defined in appendix A.)

The band on the figure is the locus of stall points obtained by using screens (ref. 7). The symbols represent the stalls obtained using the air-jet system. A  $180^\circ$  distortion was used for both sets of data (i. e., a  $180^\circ$  screen sector and three  $60^\circ$  air-jet sectors were used). The predicted limit for this engine is shown by the dashed line. Good agreement exists between the screen and jet data. The data are also considered to be in relatively good agreement with the prediction, inasmuch as it was predicted from sea-level test data adjusted for the particular engine and the 0.5 Reynolds number index flight condition. The uncertainty of the  $K_{D2}$  parameter due to the difficulty in accurately determining the area of pressure below the average with only 40 pressure measurements is approximately 50 units. The 100 units between the predicted and observed limits are typical of this type of data.

Total pressure contours obtained with screen and air-jet distortions which cause compressor stall are compared in figure 14. The contours represent constant values of the difference between the average and local total pressure as a percentage of the average pressure. A sharper gradient at the edge of the distortion is observed for the screen-induced distortion. This is also observed in the pressure profile presented in figure 15. Here the ratio of the radially averaged total pressure to the face average pressure is presented as a function of circumferential position. It can also be noted that the levels were very similar for the two sets of data, the major difference being the apparent gradients at the edge of the distortion. This resulted in only a small variation in  $K_{D2}$ .

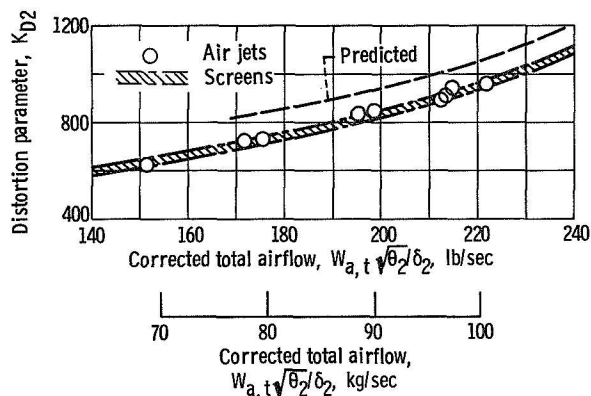
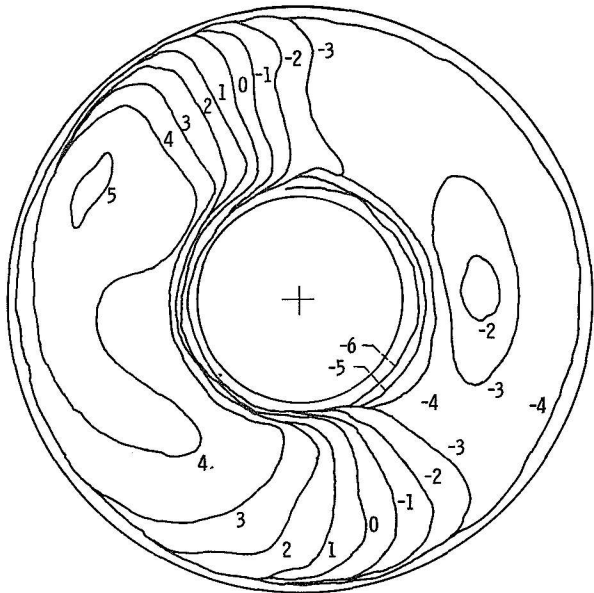


Figure 13. - Comparison of stall limits with air-jet and screen-induced 180° distortion. Reynolds number index, 0.5; exhaust nozzle area,  $A_j = 100$  percent of rated area.

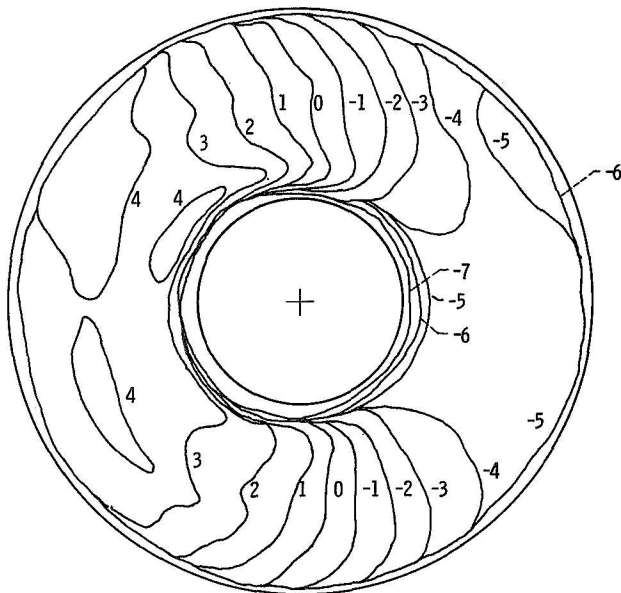
The Mach number contours for the screen- and air-jet-induced distortion are compared in figure 16 and the circumferential profiles in figure 15(b). The contours exhibit similar trends for the screen and air-jet distortions, the range being approximately one-tenth of a Mach number. The circumferential profile indicates that the screens had a sharper transition from the undistorted to distorted side than the air jets. There is also indicated an increase in Mach number just ahead of the edge of the distortion and a depression just behind the edge. However, closer circumferentially spaced probes would be required to accurately define the profile in this area. This trend is similar to those discussed in references 2 and 7.

The preceding comparison between the screens and air jets in producing an 180° distortion was made at a relatively low distortion and airflow, where comparable data exist. A set of contours nearer to rated conditions is presented in figure 17. This is again a distortion that caused the engine to stall. The  $K_{D2}$  is correspondingly larger and the edges less well defined than for the lower flow case of figure 14, and the range in total pressure is  $\pm 5$  percent compared to  $\pm 4$  percent. The Mach number profiles indicate a similar range in Mach numbers, 0.1, but the level is higher, 0.4 compared to 0.3. This corresponds to increasing the flow into the engine from 176 to 215 pounds per second (79.9 to 97.5 kg/sec). The small Mach number gradient is consistent with the uniform velocity concept (ref. 7), where the compressor tries to minimize velocity distortions.

Also included in figure 17 are contours of the TRMS pressure amplitude. These values range from 0.4 to 1.3 percent of the mean local pressure (i.e., the "steady-state" value as measured by the adjacent steady-state probe). These values are for the 0- to 500-hertz band but are based on 40 transducer readings instead of 18, as mentioned previously. There does not seem to be any consistent relation between the higher values and jet locations.



(a) Screen distortion;  $K_{D2} = 683$ .



(b) Air-jet distortion; distortion factor,  $K_{D2} = 726$ .

Figure 14. - Total pressure distributions at compressor face with air-jet- and screen-induced  $180^\circ$  distortion. Reynolds number index, 0.5; corrected total airflow, 176 pounds per second (80 kg/sec).

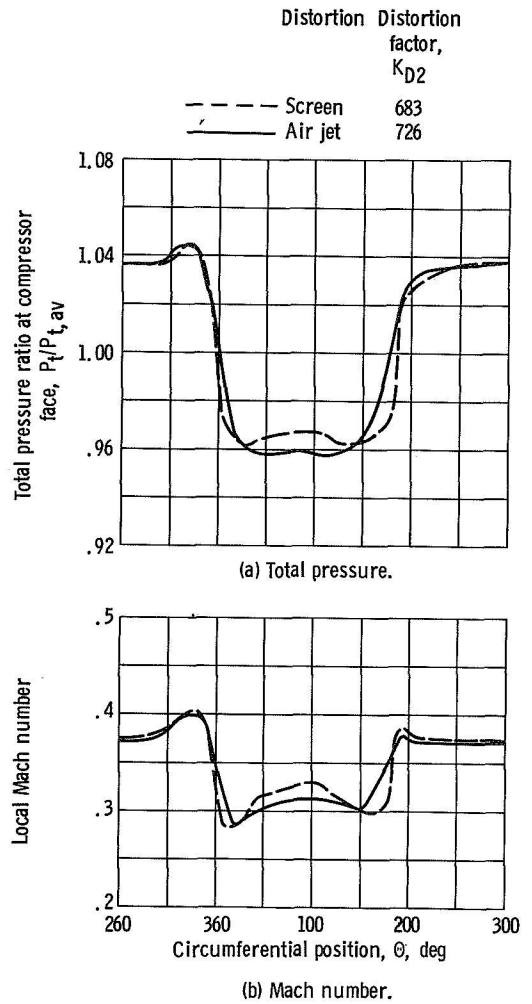
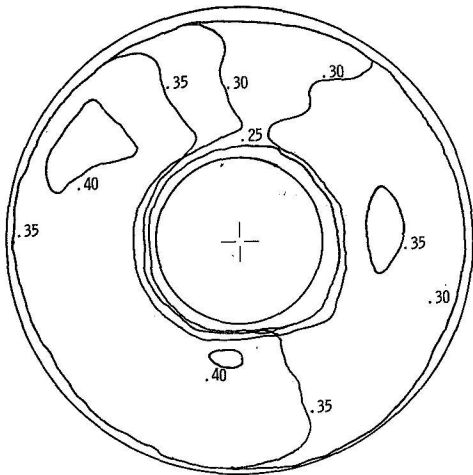
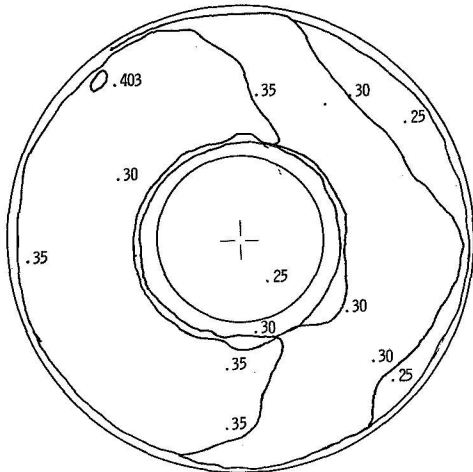


Figure 15. - Circumferential total pressure profiles at compressor inlet with air-jet- and screen-induced  $180^\circ$  distortion. Corrected total airflow,  $W_a t \sqrt{\theta_2/\delta_2} = 176$  pounds per second (80 kg/sec).

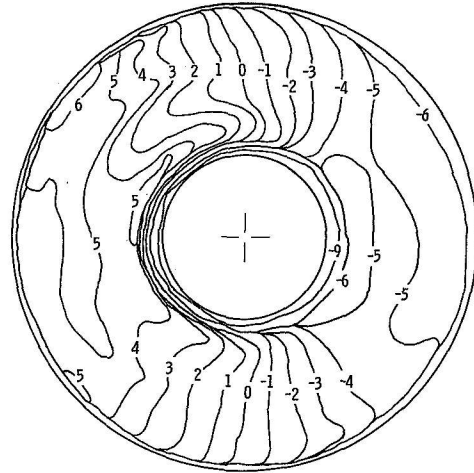


(a) Screen distortion; distortion factor,  $K_{D2} = 683$ .

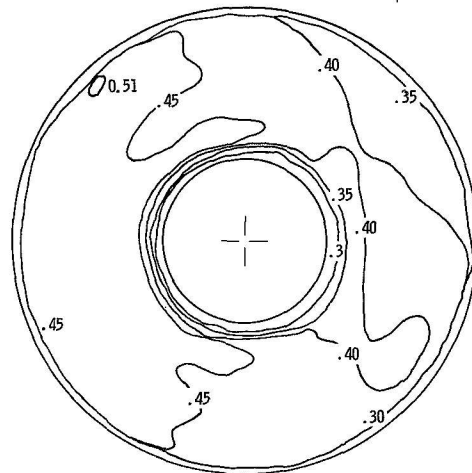


(b) Air-jet distortion; distortion factor,  $K_{D2} = 726$ .

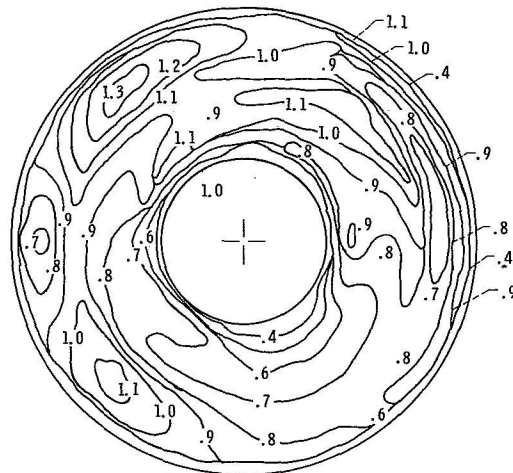
Figure 16. - Mach number distribution at compressor face with air-jet- and screen-induced 180° distortion. Corrected total airflow,  $W_{a,t} \sqrt{\theta_2} / \delta_2 = 176$  pounds per second (80 kg/sec).



(a) Total pressure,  $(P_{av} - P) / P_{av}$ .



(b) Mach number.



(c) TRMS amplitude,  $\Delta P_{TRMS} / P_{mean}$ ; average  $\Delta P_{TRMS} / P_{mean}$ , 0.7 percent.

Figure 17. - Inlet contours of air-jet-induced 180° distortions. Corrected total airflow, 215 pounds per second (98 kg/sec); distortion factor,  $K_{D2} = 946$ .

## SUMMARY OF RESULTS

A more versatile method of creating compressor inlet distortions has been developed at Lewis Research Center. The effect on compressor performance of the air-jet system is compared to that of the conventional screens. This investigation was conducted on a nonstandard TF30-P-1 turbofan engine at an inlet Reynolds number index of 0.5 for an  $180^\circ$  total pressure distortion.

1. The presence of the air-jet system, with and without uniform secondary flow through the jets, had little effect on the pressure distribution or the random pressure fluctuations.

2. The momentum pressure loss is primarily a function of the jet pressure (i.e., secondary airflow through the jets), and only very slightly a function of the total airflow into the compressor. Therefore a relatively constant distortion can be maintained over a range of engine speeds.

3. The air jets produce distortions similar to those produced by screens, with only slightly greater spreading at the edge of the distortion patterns. The stall-limited distortions, determined with screens and air jets, were in good agreement.

4. The distribution of TRMS pressure amplitude does not show any significant relation to the jets or distortion pattern.

Lewis Research Center,  
National Aeronautics and Space Administration,  
Cleveland, Ohio, October 24, 1969,  
720-03.

# APPENDIX A

## SYMBOLS

A	flow area, ft <sup>2</sup> (cm <sup>2</sup> )	$\delta$	ratio of total pressure to standard sea-level static pressure
C	constant		
D	mean diameter, in. (cm)	$\Theta$	circumferential position, deg
$K_{D2}$	Pratt & Whitney distortion factor (see appendix B)	$\theta$	ratio of total temperature to standard sea-level static temperature
$N_1$	low-rotor speed, rpm		
$N_2$	high-rotor speed, rpm		
P	static pressure, psi (N/cm <sup>2</sup> )	$\mu$	absolute viscosity, (N-sec)/m <sup>2</sup>
$P_t$	total pressure, psi (N/cm <sup>2</sup> )	Subscripts:	
R	gas constant, 53.3 (ft-lb)/(lb)(°R), 286 J/(kg)(K)	1, . . . , 10	instrumentation station locations
RNI	Reynolds number index, $\delta / \left( \frac{\mu}{\mu_{sl}} \right) \sqrt{\theta}$	a	absolute
		av	average
		c	core
T	total temperature, °R (K)	f	fan duct
$W_a$	airflow rate, lb/sec (kg/sec)	j	exhaust nozzle
		r	ring
$W_s$	secondary weight flow, lb/sec (kg/sec)	sl	sea level
		t	total condition
$\Delta$	difference between values	vd	flow control valve discharge (air jet)

## APPENDIX B

### DEFINITIONS

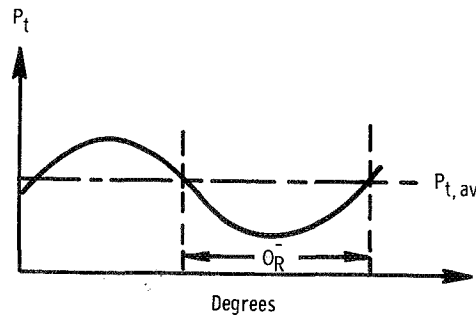
#### Pratt & Whitney Distortion Factor, $K_{D2}$

The distortion parameter  $K_{D2}$  is defined by the following equation:

$$K_{D2} = \frac{\sum_{r=1}^n \Theta_r^- \left( \frac{\Delta P}{P} \right)_r \frac{OD}{D_r}}{\sum_{r=1}^n \frac{OD}{D_r}}$$

The terms appearing in the equation for  $K_{D2}$  are defined as follows:

- r            a particular ring of total pressure probes
- $\Theta_r^-$         circumferential extent of largest single pressure depression below  $P_{t,av}$  in degrees, for a particular ring (see following sketch)
- $\left( \frac{\Delta P}{P} \right)_r$      $\frac{P_{t,av} - P_{t,min}}{P_{t,av}}$ , in percent, for a particular ring
- $P_{t,av}$         average pressure per ring
- $P_{t,min}$        minimum pressure per ring
- OD            outer diameter of duct
- $D_r$            diameter of a particular ring
- n              number of measurement rings



## Compressor Efficiency

The compressor efficiency is defined as the ratio of isentropic enthalpy rise to the actual enthalpy rise across the compressor unit or stage grouping.

## TRMS Pressure Amplitude

After the signal from a high-response pressure transducer has been passed through a low-pass filter set to 500 hertz (a frequency below one-fourth the resonance frequency of the probes used), it is fed into a TRMS meter. The TRMS meter indicates the true root mean square of the amplitude of the transducer signal which is equivalent to the standard deviation  $\sigma$  of the pressure fluctuations. This standard deviation is expressed as a percentage of the mean pressure level as measured by adjacent steady-state (very low response) instrumentation.

## APPENDIX C

### HIGH-RESPONSE INSTRUMENTATION

#### Probe Design

Due to the nature of the research program, it was necessary to utilize high-response instrumentation that had the capability of reliably measuring pressure variations of 300 hertz with a maximum amplitude error of  $\pm 5$  percent. To meet this requirement, miniature 1/4-inch (0.64-cm) diameter pressure transducers, which can be mounted in the pressure rake body itself, were used, as discussed in reference 5. This feature makes it possible for the transducers to be short-coupled (1 to 2 in.) to their sensing points in the gas stream. Because the transducers were limited to a  $170^{\circ}$  F ( $76.5^{\circ}$  C) operating temperature and had significant calibration shifts with temperature changes, water cooling was employed. The transducers, mounted in the water jackets, could be removed for repair without removing the complete rake from the engine. Typical probe installations are shown in figure 18.

Due to the design requirements of the probes, some of the coupling lengths were longer than desired. The following table shows the coupling lengths and frequency response of the probes for various instrumentation locations throughout the engine:

Station	Coupling length		Response, Hz
	in.	cm	
2	1.45	3.68	375
2.3f	2.25	5.71	220
2.3	2.20	5.59	230
2.6	2.25	5.71	220
3	1.60	4.06	350
3.12	1.35	3.43	415
4	2.50	6.35	190

#### Calibration System

Preliminary calibration of these miniature transducers indicated that zero and sensitivity shifts occurred as a function of time and were not predictable. Thus, it was not possible to trust the prerun calibrations for any extended period of time. Therefore, a system was devised to calibrate these transducers in their operating environment inside the engine just prior to recording transient data. These transducers were only used to

measure the pressure change from the steady-state values existing just prior to the transient. A schematic of the calibration system is shown in figure 19.

The calibration of these miniature  $\Delta P$  transducers consisted of observing the

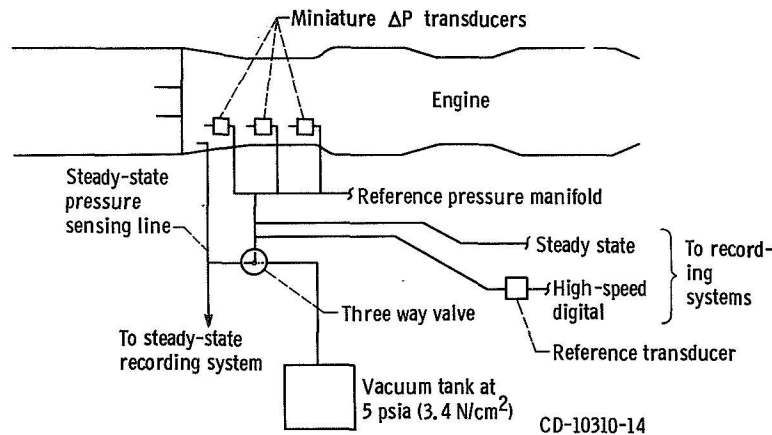
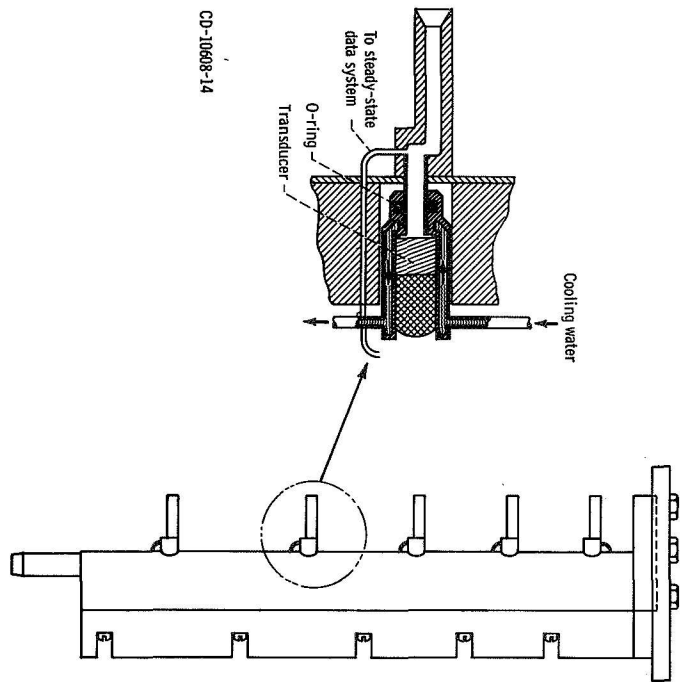


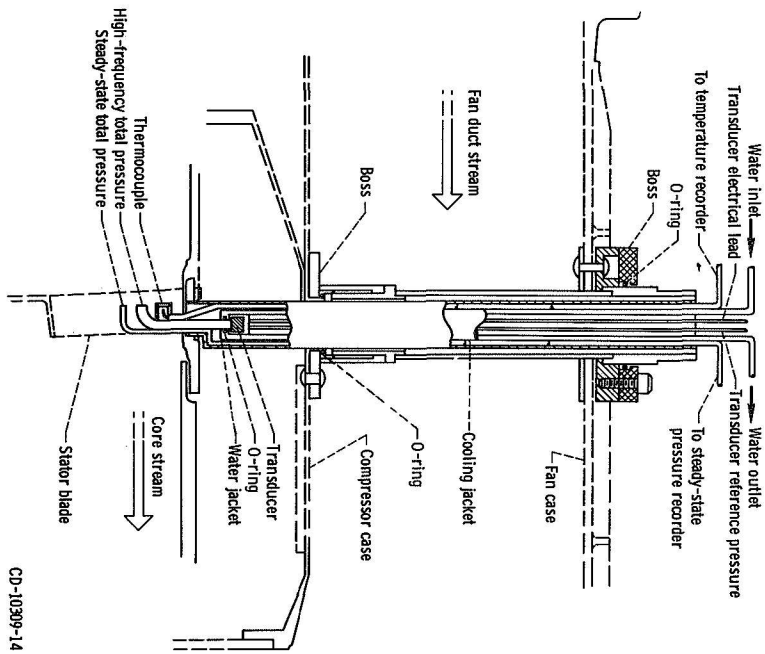
Figure 19. - Reference system used for transient instrumentation calibration.

change in output for two values of reference pressure. The engine pressures were held constant by maintaining steady-state conditions. One reference pressure was a constant of approximately 5 psia (3.4 N/cm<sup>2</sup> abs). The second reference pressure was obtained from the engine by using the normal steady-state pressure probes. The transducer reference pressure lines were connected to reference manifolds. There were four such manifolds, each using a different engine pressure level as a reference. Three-way valves were utilized to connect first the constant 5-psia (3.4-N/cm<sup>2</sup> abs) pressure and then the engine pressures to the reference manifolds to establish the calibration sequence. The sensitivity of the transducers is the ratio of the change in reference pressure to the change in transducer output. The second, or engine, pressure was maintained constant during the transient. The base pressure levels for these transient measurements were obtained from an adjacent steady-state pressure measurement.

The high-frequency response data were recorded simultaneously on a high-speed digitizer-recorder and on magnetic tape. The digital recorder had a sampling rate of approximately 50 samples per second per channel. Therefore, these data were used only to follow the transient up to the point of stall. The actual stall point and time sequence were obtained from the analog traces made from the magnetic tape.



(a) Compressor inlet rake.



(b) Interstage probe.

Figure 18 - Typical probe installation.

## REFERENCES

1. Winslow, Larry J.; Wendland, Daniel W.; Smith, Brian D.; Welliver, Albertus D.: Inlet Distortion Investigation - Upstream Engine Influence and Screen Simulation. Boeing Co. (AFAPL-TR-68-140, DDC No. AD-847095), Jan. 1969.
2. Langston, C. E.: Distortion Tolerance - By Design Instead of by Accident. Paper 69-GT-115, ASME, Mar. 1969.
3. Reid, C.: The Response of Axial Flow Compressors to Intake Flow Distortion. Paper 69-GT-29, ASME, Mar. 1969.
4. Bellman, Donald R.; and Hughes, Donald L.: The Flight Investigation of Pressure Phenomena in the Air Intake of an F-111A Airplane. Paper 69-488, AIAA, June 1969.
5. Braithwaite, Willis M.; and Vollmar, William R.: Performance and Stall Limits of a YTF30-P-1 Turbofan Engine with Uniform Inlet Flow. NASA TM X-1803, 1969.
6. Meyer, Carl L.; McAulay, John E.; and Biesiadny, Thomas J.: Technique for Inducing Controlled Steady-State and Dynamic Inlet Pressure Disturbances for Jet Engine Tests. NASA TM X-1946, 1970.
7. Werner, Roger A.; Abdelwahab, Mahmood; and Braithwaite, Willis M.: Performance and Stall Limits of an Afterburner-Equipped Turbofan Engine with Inlet Flow Distortion. NASA TM X-1947, 1970.
8. Staff of Lewis Laboratory: Central Automatic Data Processing System. NACA TN 4212, 1958.
9. Mechtly, E. A.: The International System of Units - Physical Constants and Conversion Factors. NASA SP-7012, 1964.



*"The aeronautical and space activities of the United States shall be conducted so as to contribute . . . to the expansion of human knowledge of phenomena in the atmosphere and space. The Administration shall provide for the widest practicable and appropriate dissemination of information concerning its activities and the results thereof."*

— NATIONAL AERONAUTICS AND SPACE ACT OF 1958

## NASA SCIENTIFIC AND TECHNICAL PUBLICATIONS

**TECHNICAL REPORTS:** Scientific and technical information considered important, complete, and a lasting contribution to existing knowledge.

**TECHNICAL NOTES:** Information less broad in scope but nevertheless of importance as a contribution to existing knowledge.

**TECHNICAL MEMORANDUMS:** Information receiving limited distribution because of preliminary data, security classification, or other reasons.

**CONTRACTOR REPORTS:** Scientific and technical information generated under a NASA contract or grant and considered an important contribution to existing knowledge.

**TECHNICAL TRANSLATIONS:** Information published in a foreign language considered to merit NASA distribution in English.

**SPECIAL PUBLICATIONS:** Information derived from or of value to NASA activities. Publications include conference proceedings, monographs, data compilations, handbooks, sourcebooks, and special bibliographies.

**TECHNOLOGY UTILIZATION PUBLICATIONS:** Information on technology used by NASA that may be of particular interest in commercial and other non-aerospace applications. Publications include Tech Briefs, Technology Utilization Reports and Notes, and Technology Surveys.

*Details on the availability of these publications may be obtained from:*

SCIENTIFIC AND TECHNICAL INFORMATION DIVISION  
NATIONAL AERONAUTICS AND SPACE ADMINISTRATION  
Washington, D.C. 20546